COMMUNICATION

Rigidochromism of Tetranuclear Cu(I)–Pyrazolate Macrocycles: Steric Crowding with Trifluoromethyl Groups

Shinaj K. Rajagopal,[a] Matthias Zeller,[a] Sergei Savikhin,[b] Lyudmila V. Slipchenko,[a] and Alexander Wei*[,a,c]

Received 00th January 20xx,
Accepted 00th January 20xx

DOI: 10.1039/x0xx00000x

Macrocyclic Cu(I)–pyrazolate tetramers (Cu_4pz_4) can fold into compact structures with luminescent Cu_4 cores whose emission wavelengths are sensitive to steric effects along the periphery of the macrocycle. Introducing CF_3 at the C4 position of 3,5-di-^{t}Bu-pyrazolate increases steric crowding that modifies the conformational behavior of the Cu_4pz_4 complex, highlighted by a low-temperature martensitic transition. Variable-temperature analysis of solid-state luminescence reveal an unexpected blueshifting of emission with rising temperature.

Introduction

Solid-state luminescence continues to be a fascinating subject, rejuvenated in recent years by interests in materials that can improve solid-state lighting efficiency,[1] or respond to external stimuli for sensor or imaging applications.[2] Among the myriad categories of luminescent materials, Cu(I) complexes have a special appeal: Copper is an earth-abundant element and has yielded a variety of photoactive materials, many of which can be made by mixing simple salts with appropriately designed organic ligands.[3,4,5,6] Recent advances include Cu(I) emitters for thermally activated delayed fluorescence (TADF),[7,8,9] circularly polarized emission from chiral Cu clusters,[10,11] and efficient radioluminescence with application in X-ray imaging.[12]

Copper(I)–pyrazolate complexes are a class of luminescent clusters that have yielded many interesting examples of solid-state luminochromism. Trinuclear Cu(I)–pyrazolates (Cu_3pz_3) have been studied extensively,[6,13] but attention is being paid more recently to tetranuclear Cu_4pz_4 species which are also highly luminescent.[14,15,16,17] One important distinction is that Cu_3pz_3 structures are planar and prone to intermolecular stacking which strongly affects their emissive states, whereas Cu_4pz_4 complexes are saddle-shaped and their emission wavelengths (λ_{em}) are unaffected by neighbouring clusters.

We recently studied a series of Cu_4pz_4 complexes prepared from 3,5-di-^{t}Bu-pyrazole and C4-substituted derivatives, whose solid-state emissions depend primarily on electronic transitions from triplet cluster-centred (^{3}CC) excited states.[16] A remarkable feature of these macrocyclic complexes is the strong impact of the C4 substituent on λ_{em}, which is steric in nature rather than electronic. For example, a tetranuclear complex made with 3,5-di-^{t}Bu-pyrazole (Cu_4(H-pz)$_4$, **1**) emits yellow light (λ_{em} 559 nm),[14] whereas a complex made with 3,5-di-^{t}Bu-4-methylpyrazole (Cu_4(Me-pz)$_4$, **2**) emits deep blue light (λ_{em} 457 nm).[16] The C4 methyl causes the flanking ^{t}Bu units to adopt bisected geometries, enabling macrocycle **2** to fold into a compact, conformationally rigid structure with the four Cu atoms compressed into a close-packed rhombus (Fig. 1, *lower right*). This geometry limits the excited-state contraction of the Cu_4 cluster, thereby supporting deep-blue emission.[16] Such long-range effects on rigidochromism motivated us to examine the influence of bulkier C4 substituents on the global conformation and photoluminescence (PL) of related Cu_4pz_4 species.

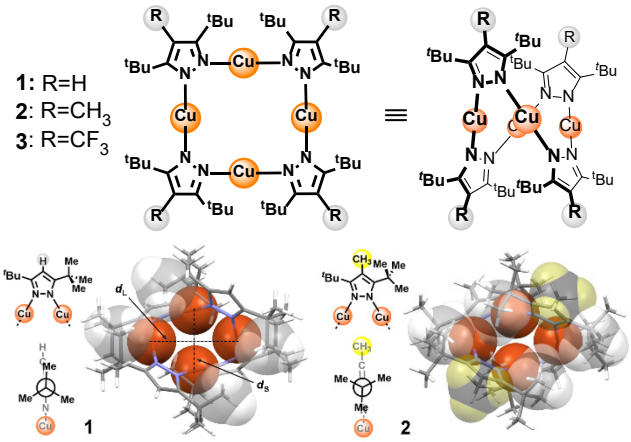

Figure 1. *Top,* Cu_4pz_4 complexes **1–3** (planar view and saddle-shaped structure). *Bottom*, top view of **1** and **2** with vdW contours for CH_3 and *endo*-methyl units in ^{t}Bu groups. The aspect ratio (d_L/d_S) of the Cu_4 rhombus is 1.43 for **1** and 1.60 for **2**; X-ray data from Ref. 16.

In this paper we describe the synthesis, structure, and PL of $Cu_4(CF_3\text{-pz})_4$ (**3**), a tetranuclear complex prepared from 3,5-di-^{t}Bu-4-trifluoromethylpyrazole (**4**). The van der Waals volume of

[a] *James and Margaret Tarpo Department of Chemistry, Purdue University, West Lafayette, Indiana 47907, USA*
[b] *Department of Physics and Astronomy, Purdue University, West Lafayette, Indiana 47907, USA*
[c] *School of Materials Engineering, Purdue University, West Lafayette, Indiana 47907, USA*

† Footnotes relating to the title and/or authors should appear here.
Electronic Supplementary Information (ESI) available: Synthesis details and chemical characterization, photophysical and x-ray crystallographic data, computational DFT and TD-DFT analysis. See DOI: 10.1039/x0xx00000x

CF_3 in **3** is nearly twice that of CH_3 in **2** (39.2 vs 21.0 Å^3) and thus expected to maintain neighbouring ^{t}Bu units in bisected conformations. However, the CF_3 groups influence solid-state behaviour in unexpected ways, including a polymorphic shift at low temperature and a high-energy PL band whose intensity *increases* with temperature for powders and thin films.

$Cu_4(CF_3\text{-pz})_4$ **3** can be formed in one step from compound **4**, which in turn can be prepared from a 4-iodopyrazole precursor (**Scheme 1**). However, the insertion of a bulky CF_3 between two ^{t}Bu units is synthetically challenging. After exploring several different methods, we found trifluoromethyl thianthrenium triflate (CF_3-TT$^+$OTf$^-$) developed by Ritter and coworkers to be an excellent CF_3 transfer agent under Cu-mediated cross-coupling conditions,[18] producing 3,5-^{t}Bu$_2$-4-CF_3-pz **4** in 88% overall yield after debenzylation (details in ESI). Pyrazole **4** was then mixed with $[Cu(CH_3CN)_4]BF_4$ in MeOH to form Cu_4pz_4 complex **3**, which precipitated as a colourless solid in 70% yield.

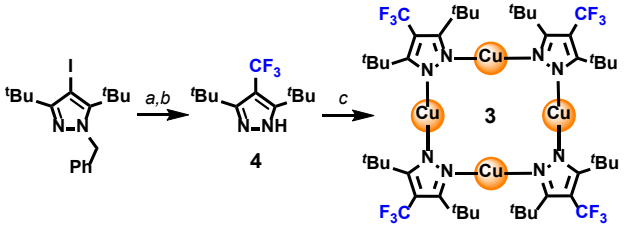

Scheme 1. Synthesis of $Cu_4(CF_3\text{-pz})_4$ (**3**). (a) TT(CF_3)OTf (2 eq), Cu^0 (3 eq), DMF, 60 °C. (b) 5% Pd/C (cat.), H_2 (1 atm), 1:1 EtOAc:MeOH, rt. (c) $[Cu(CH_3CN)_4]BF_4$ (1 eq), Et_3N (1 eq), MeOH, rt.

$Cu_4(CF_3\text{-pz})_4$ **3** produces a brilliant green luminescence in the solid state with a quantum yield of 42% and decay lifetime of 27.6 μs at 300 K, indicating room-temperature phosphorescence (Fig. S1, Table S1, ESI). The PL spectrum of **3** at 295 K in powder form shows a peak λ_{em} centred at 519 nm, plus a shoulder at roughly 450 nm that is amplified and broadened in thin film samples (Fig. 2a). Excitation spectra corresponding with each emission band both show a broad peak at 280 nm (Fig. S2), a signature of the $S_0 \rightarrow T_1$ transition for ^{3}CC states.[15] DFT calculations of **3** confirm that the HOMO–LUMO transition is controlled through CC orbitals (Fig. 2b). The primary role of ^{3}CC states in Cu_4pz_4 emission is remarkable, given its history as a secondary, low-energy pathway in other Cu(I) clusters.[3,19]

The green luminescence of **3** is contrary to our initial expectations, as the role of steric bulk at C4 in enforcing the conformational rigidity of Cu_4pz_4 has been shown with smaller substituents (R=Cl, Br, and CH_3), all having λ_{em} < 460 nm.[16] We thus considered whether the CF_3 group was sufficiently large to (i) cause distortions in the pyrazole ring by creating torsional strain between neighbouring ^{t}Bu groups, and (ii) direct transannular interactions between opposing pyrazolate ligands that prevent Cu atoms from adopting a close-packed geometry.

X-ray analysis of crystals grown from a toluene/CH_2Cl_2 solution of **3** confirms that the $Cu_4(CF_3\text{-pz})_4$ macrocycle adopts a saddle-shaped conformation (Fig. 3a). Analysis at 150 K yields a triclinic unit cell containing two sets of four independent structures, each with a slightly different conformation but otherwise adopting the same folded geometry (Fig. 3b,c). However, whereas the Cu_4 core of $Cu_4(Me\text{-pz})_4$ **2** is a planar, close-packed rhombus with a large aspect ratio (d_L/d_S = 1.60; Fig. 1),[16] the Cu atoms of **3** form nonplanar quadrangles with low aspect ratios (1.03–1.16).

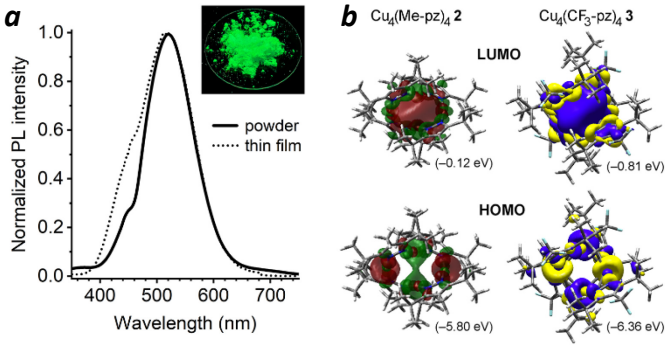

Figure 2. (a) PL spectra of $Cu_4(CF_3\text{-Pz})_4$ **3** in powder and thin-film forms (λ_{ex} 270 nm, peak λ_{em} 519 nm); *inset*, luminescent powder using 254-nm excitation. (b) DFT analysis of $Cu_4(Me\text{-Pz})_4$ **2** and $Cu_4(CF_3\text{-Pz})_4$ **3** with HOMO and LUMO structures and energies; analysis of **2** is described in Ref. 16.

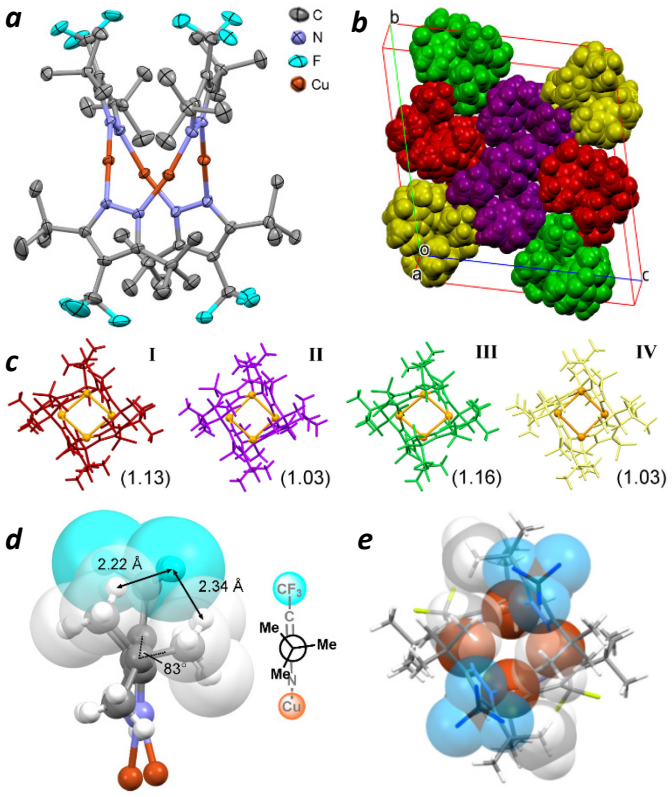

Figure 3. (a) X-ray crystal structure of **3** (Conformer **I**) at 150 K; thermal ellipsoids drawn at the 50% probability level with H atoms removed for clarity; see Fig. S5 for other conformers. (b,c) Triclinic unit cell of $Cu_4(CF_3\text{-Pz})_4$ **3** at 150 K with conformers **I**–**IV**; Cu_4 quadrangle drawn in orange with d_L/d_S in parentheses. (d) Edge view of CF_3-pz showing select F···H distances and dihedral angle of protruding CH_3. (e) Top view of **3** (conformer **I**) with vdW contours for CF_3 groups and *endo*-methyl units in ^{t}Bu groups.

A close inspection of the pyrazolate ligands in **3** reveals that the CF_3 is tightly wedged against adjacent ^{t}Bu groups with nearest-neighbour F···H distances of 2.15–2.35 Å, much shorter than the sum of their vdW radii (2.6–2.7 Å).[20] Torsional strain is reduced by (i) bending ^{t}Bu groups out of plane by up to 10° and (ii) rotating their methyl units 12–24° away from their ideal bisected conformations (ϕ=60°), with one unit projected nearly

normal to the pyrazole ring (Fig. 3d). These distortions reflect the sizable allylic strain imposed on the ^{t}Bu units by CF_3.

^{t}Bu methyl groups that project inward (*endo*) perturb the conformation of the Cu_4pz_4 macrocycle. To reduce transannular steric interactions, the pyrazolate ligands twist so that each face is positioned directly across an opposing ^{t}Bu unit, resulting in the interdigitation of *endo* methyls (Fig. 3e). The twisting of pyrazolate rings causes the Cu_4 quadrangles to buckle with bend angles of 27.4–32.9° (Fig. 3a and S8, Table S2), and creates a sizable gap in the Cu_4 core of **3** with d_S values of 3.65–3.90 Å. In comparison, the Cu_4 rhombus of **2** has a bend angle of 0° with d_S of 3.05 Å (Fig. 1, Table S2).

The λ_{em} peak at 519 nm for **3** (Fig. 2a) is in accord with other luminescent Cu_4pz_4 complexes with nonplanar Cu_4 cores.[14–16] We have noted previously that Cu atom mobility promotes excited-state contraction and can induce a redshift in Cu_4pz_4 emission.[16] In the case of complex **3**, the presence of several conformers in the unit cell at 150 K indicates that the Cu_4pz_4 macrocycle can adopt multiple low-energy structures, with DFT calculations of conformers **I**–**IV** suggesting $\Delta\Delta H_0$ <1 kcal/mol (Table S5). Although all Cu_4pz_4 conformations are stabilized by the interdigitation of ^{t}Bu groups, time-dependent (TD) DFT analysis of their ground (S_0) and first excited triplet (T_1) states reveals very similar degrees of excited-state contraction by the Cu_4 core (Fig. S9, S10), confirming the importance of Cu-atom close packing in the rigidochromism of Cu_4pz_4 complexes.[16]

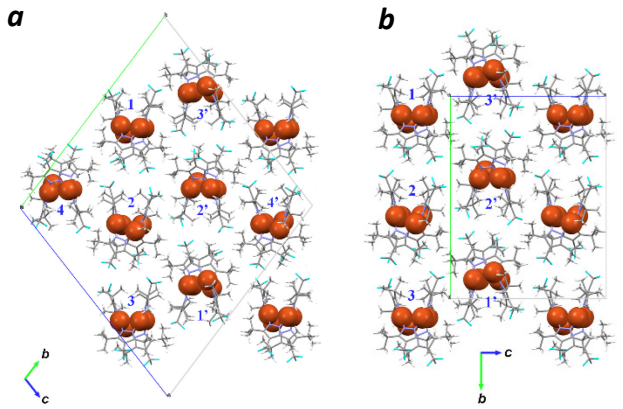

Figure 4. (a) Triclinic unit cell for **3** at 150 K (*P*-1; ***a*** 10.75 ***b*** 33.09 ***c*** 33.10 Å; **α** 104.1 **β** 95.6 **γ** 95.6°; ***V*** 11278.5 Å^3). (b) monoclinic unit cell for **3** at 200 K ($P2_1/c$; ***a*** 10.81 ***b*** 26.11 ***c*** 20.43 Å; **α** 90 **β** 99.0 **γ** 90°; ***V*** 5695.8 Å^3). Both cells are viewed along the *a* axis.

Gradual warming of **3** between 150 and 200 K induces a martensitic transition from a triclinic (*P*-1) to monoclinic lattice ($P2_1/c$; Fig. 4). X-ray analysis at 200 K shows a single conformer with some rotational disorder in the CF_3 and ^{t}Bu groups (Fig. S6). The distance between Cu_4 centroids along the [01-1] direction at 150 K (13.45 Å) decreases by 1.1% in the [010] direction at 200 K and the separation of lattice planes along [001] increases by 4%, along with minor changes in Euler angles (Table 1). The Cu_4 quadrangle at 200 K has a fixed aspect ratio of 1.07 and bend angle of 28°, and a macrocyclic conformation similar to those of **I**–**IV** (RMS deviations of 0.05–0.19 Å). Further analysis of the static disorder at 200 K suggests that CF_3 reorientation drives the librational exchange of its neighbouring ^{t}Bu groups (Fig. S7). In addition to the low-temperature polymorphic shift, reversible phase transitions were recorded by differential scanning calorimetry at 170 and 200 K (Fig. S11).

Table 1 Centroid distances and angles for crystalline lattices of **3** at 150 and 200 K

Parameters	150 K	200 K[a]
Centroid distances (Å)		
1–2	13.53	13.28
2–3	13.36	13.28
2–2'	11.61	11.40
Euler angles (deg.)		
1–2–2'	60.7	61.8
3–2–2'	114.8	116.8
1–2–3	162.6	159.0

[a] All Cu_4pz_4 clusters have equivalent conformations at 200 K.

To determine whether low-temperature phase transitions might influence solid-state emission, variable-temperature PL studies were performed on powder and thin-film samples of **3** (Fig. 5). Both samples produce strong and well-defined emission bands at 77 K (λ_{em} 532–537 nm); minor peaks in the violet region (400–415 nm) are also observed. The main PL band broadens and blueshifts upon warming to 300 K (513–518 nm), accompanied by a notable increase of a secondary PL band in the blue region (420–480 nm).

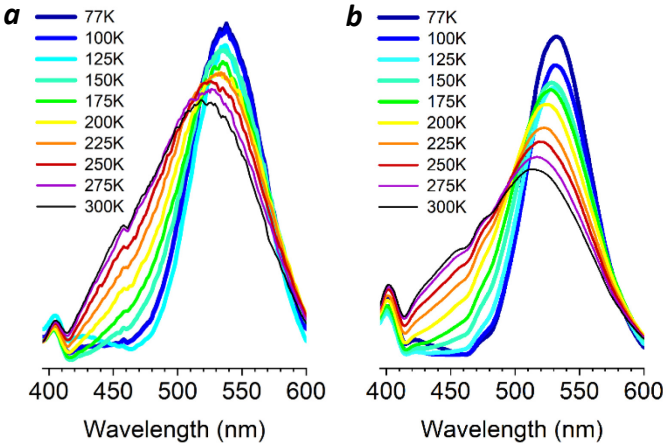

Figure 5. Variable-temperature PL spectra of **3** in the solid state. (a) Powder in borosilicate glass tube (λ_{ex} 300 nm); (b) thin film on quartz (λ_{ex} 270 nm).

The higher energy PL band is curious and may be related to the lowering of excited-state energies by the strongly electronegative CF_3 group. Variable-temperature analysis of PL lifetimes indicates a modest decrease in τ at 450 nm and no changes at 520 or 532 nm with rising temperature, ruling out the possibility of TADF (Figure S5). We postulate that complex **3** in these samples adopts numerous conformations at domain interfaces or in amorphous regions. The distribution of states can increase from several conformers below 150 K to a multitude of conformations above 200 K, with an increasing number of close-packed Cu_4 clusters that support blue emission.[16] While the distributions are under thermodynamic control, the solid-state conformations are kinetically stable on the microsecond timescale and support varying degrees of rigidochromism based on their ground-state structures.

In conclusion, introducing CF_3 between two ^{t}Bu groups on a trisubstituted pyrazole generates steric crowding that impacts the conformational and luminescence behavior of the Cu_4pz_4 macrocycle. Whereas C4-CH_3 units drive neighbouring ^{t}Bu groups into bisected rotamers that result in a compact Cu_4pz_4 conformation with nearly close-packed Cu atoms,[16] C4-CF_3 units distort local geometries that produce competing steric effects and a gap in the Cu_4 core. Overall we find that the rigidochromism of Cu_4pz_4 is best reinforced by C4 substituents of intermediate size, to support conformations that minimize excited-state reorganization of the Cu_4 cluster.

Author Contributions

S.K.R.: synthesis, PL studies, DFT analysis; M.Z.: x-ray crystallography; S.S.: PL training; L.V.S.: DFT supervision; A.W.: research design. S.K.R. and A.W. wrote the manuscript.

Data availability

Supplementary crystallographic data (CCDC 2370073, 2370077) can be obtained free of charge (www.ccdc.cam.ac.uk/data_request/cif). Other data will be made available on request.

Conflicts of interest

There are no conflicts to declare.

Acknowledgements

We thank the US National Science Foundation (CHE-2102639, CHE-2204206), Dept. of Energy (DE-SC0018239), NIH (P30-CA023168), and Yuichiro Watanabe for discussions. Research was also partly supported through computational resources provided by Information Technology at Purdue University.

Notes and references

1 [1] G. Hong, X. Gan, C. Leonhardt, Z. Zhang, J. Seibert, J. M. Busch and S. Bräse, *Adv. Mater.*, 2021, **33**, 2005630.
2 [2] P. Bamfield and M. Hutchings, *Chromic Phenomena - Technological Applications of Colour Chemistry*, Royal Society of Chemistry (RSC), 3rd edn., 2018.
3 [3](a) P. C. Ford, E. Cariati and J. Bourassa, *Chem. Rev.*, 1999, **99**, 3625-3648; (b) E. Cariati, E. Lucenti, C. Botta, U. Giovanella, D. Marinotto and S. Righetto, *Coord. Chem. Rev.*, 2016, **306**, 566-614.
4 [4] M. A. Halcrow, *Dalton Trans.* **2009**, 2059-2073.
5 [5] (a) L. P. Ravaro, K. P. S. Zanoni and A. S. S. de Camargo, *Energ. Rep.*, 2020, **6**, 37-45. (b) V. K.-M. Au, *Energ. Fuels*, 2021, **35**, 18982-18999.
6 [6] J. Zheng, Z. Lu, K. Wu, G.-H. Ning and D. Li, *Chem. Rev.*, 2020, **120**, 9675-9742.
7 [7] R. Hamze, J. L. Peltier, D. Sylvinson, M. Jung, J. Cardenas, R. Haiges, M. Soleilhavoup, R. Jazzar, P. I. Djurovich, G. Bertrand and M. E. Thompson, *Science*, 2019, **363**, 601-606.
8 [8] H.-J. Wang, Y. Liu, B. Yu, S.-Q. Song, Y.-X. Zheng, K. Liu, P. Chen, H. Wang, J. Jiang, T.-Y. Li, *Angew. Chem. Int. Ed.* **2023**, 62, e202217195.
9 [9] H.-J. Wang, Y. Liu, B. Yu, S.-Q. Song, Y.-X. Zheng, K. Liu, P. Chen, H. Wang, J. Jiang and T.-Y. Li, *Angew. Chem. Int. Ed.*, 2023, **62**, e202217195.
10 [10] C. Dutta, S. Maniappan and J. Kumar, *Chem. Sci.*, 2023, **14**, 5593-5601.
11 [11] X.-H. Ma, Y. Si, J.-H. Hu, X.-Y. Dong, G. Xie, F. Pan, Y.-L. Wei, S.-Q. Zang and Y. Zhao, *J. Am. Chem. Soc.*, 2023, **145**, 25874-25886.
12 [12] Y. Wang, W. Zhao, Y. Guo, W. Hu, C. Peng, L. Li, Y. Wei, Z. Wu, W. Xu, X. Li, Y. D. Suh, X. Liu and W. Huang, *Light Sci. Appl.*, 2023, **12**, 155.
13 [13] (a) I. Boldog, E. B. Rusanov, J. Sieler, S. Blaurock and K. V. Domasevitch, *Chem. Commun.*, 2003, 740-741; (b) M. A. Rawashdeh-Omary, *Comments Inorg. Chem.* 2012, **33**, 88-101; (c) A. A. Titov, O. A. Filippov, L. M. Epstein, N. V. Belkova and E. S. Shubina, *Inorg. Chim. Acta*, 2018, **470**, 22-35. (d) A. A. Titov, V. A. Larionov, A. F. Smol'yakov, M. I. Godovikova, E. M. Titova, V. I. Maleev and E. S. Shubina, *Chem. Commun.*, 2019, **55**, 290-293.
14 [14] K. Fujisawa, Y. Ishikawa, Y. Miyashita and K.-i. Okamoto, *Inorg. Chim. Acta*, 2010, **363**, 2977-2989.
15 [15] H. V. R. Dias, H. V. K. Diyabalanage, M. M. Ghimire, J. M. Hudson, D. Parasar, C. S. Palehepitiya Gamage, S. Li and M. A. Omary, *Dalton Trans.*, 2019, **48**, 14979-14983.
16 [16] Y. Watanabe, B. M. Washer, M. Zeller, S. Savikhin, L. Slipchenko and A. Wei, *J. Am. Chem. Soc.*, 2022, **144**, 10186–10192.
17 [17] R. A. Smith, R. Kulmaczewski and M. A. Halcrow, *Inorg. Chem.*, 2023, **62**, 9300-9305.
18 [18] H. Jia, A. P. Häring, F. Berger, L. Zhang and T. Ritter, *J. Am. Chem. Soc.*, 2021, **143**, 7623-7628.
19 [19] M. Xie, C. Han, Q. Liang, J. Zhang, G. Xie and H. Xu, *Sci. Adv.*, 2019, **5**, eaav9857.
20 [20] A. Bondi, *J. Phys. Chem.*, 1964, **68**, 441-451.

